

# A KINETIC STUDY ON THE PHOTODYNAMIC PROPERTIES OF THE XANTHENE DYE MERBROMIN (MERCUROCHROME) AND ITS AGGREGATES WITH AMINO ACIDS IN AQUEOUS SOLUTION\*

Gabriela Martínez, Sonia G. Bertolotti, Oscar E. Zimerman and Norman A. García

Departamento de Química y Física - Universidad Nacional de Río Cuarto, 5800 Río Cuarto - Córdoba - Argentina

Daniel O. Mártire, Silvia E. Braslavsky\*

Max-Planck-Institut für Strahlenchemie - Postfach 101365, D-45413 Mülheim an der Ruhr - Germany

The photophysical properties and the photobleaching of the xanthene dye merbromin (MR), as well as the production and quenching of singlet molecular oxygen,  $O_2(^1\Delta_g)$ , were investigated in aqueous solutions, in comparison with the xanthene dyes eosine (Eos) and rose bengal (RB). MR photobleaches in the absence of  $O_2$  in a process involving the solvent ( $H_2O$  or alcohols). No participation of  $O_2^{\dot{}}$  or  $O_2(^1\Delta_g)$  could be established in the presence of  $O_2$ , although  $O_2$  is consumed.

In aqueous and alcoholic solutions, MR forms ground state charge transfer (CT) complexes with biologically relevant electron donor amino acids, such as histidine, thryptophan, and other indolic derivatives. These complexes are formed with relatively high association constants ( $3 \times 10^3 - 5 \times 10^3$ ) and are mainly responsible for the photobleaching of MR and the amino acids in these solutions by a mechanism involving  $O_2(^1\Delta_g)$  generated probably by an excited state of the CT complex. MR generates  $O_2(^1\Delta_g)$  with a relatively high yield ( $\Phi_A = 0.23 \pm 0.04$ ) and quenches  $O_2(^1\Delta_g)$  only physically with  $k_q = (2.3 \pm 0.05) 10^8 M^{-1} s^{-1}$ . This process does not affect the photosensitizing ability of MR under the low concentrations needed for its action. Non-donor compounds like the amino acid methionine and linoleic acid methyl ester are photodegraded by a Type II mechanism without implication of a dye CT complex.

**Keywords:** merbromin; mercurochrome; amino acids; photodynamic; xanthene dyes; photooxidation.

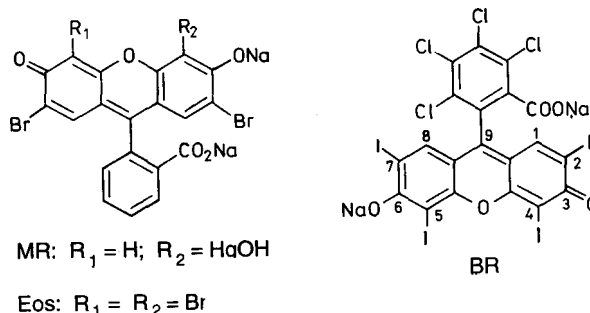
## 1. INTRODUCTION

Dye-sensitized photooxidations are being increasingly investigated due to their importance in photobiology and photomedicine.<sup>1,2</sup> In these domains, probably the most frequently studied photoreactions are those mediated by singlet molecular oxygen,  $O_2(^1\Delta_g)$ ,<sup>2,3</sup> through a Type II process. This constitutes the most important feature of photodynamic action, which comprises the damaging effects in biological assemblies by visible light in the presence of a dye sensitizer and molecular oxygen.<sup>4</sup>

In the last years, several soluble and insoluble, natural as well as synthetic photoactive materials have been analysed in connection with photodynamic action. Among them, xanthene dyes, especially the fluorescein derivative rose bengal (RB), have been widely studied.<sup>5</sup> Recently, Gollnick *et al.* published two reports on the sensitizing properties of the xanthene dye merbromin (MR).<sup>6,7</sup> Triplet quantum yields ( $\Phi_T$ ) and quantum yields for  $O_2(^1\Delta_g)$  generation ( $\Phi_A$ ) were reported in a comparative study with several fluorescein dyes.<sup>7</sup> The authors showed that MR, a mercury-substituted dibromo derivative of fluorescein, widely used as an external inexpensive antiseptic, is a relatively efficient sensitizer in alcoholic solutions.<sup>7</sup> Such observations may have clinical relevance in relation to potential photoreactions generated upon exposure of MR to daylight. For this reason, we found interesting to go further in the investigation of the sensitizing properties of MR in aqueous solution.

One possible approach to this problem is the analysis of reaction kinetics and mechanisms involved in the photooxidation

events. In the present contribution we evaluate the relative importance of the different steps in MR photophysics and aerobic photochemistry under sensitizing conditions and in the presence of biologically relevant substrates.



## 2. MATERIALS AND METHODS

### 2.1 Chemicals

L-methionine (met), L-tryptophan (trp), L-histidine (his), L-alanine (ala), L-glycine (gly), glycyl-L-tryptophan (gly-trp) and linoleic acid methyl ester (linoME) were from Sigma and used without further purification. Rose bengal (RB), eosine (Eos), and anthracene-methanol (AM) (Aldrich) were recrystallized from methanol. Zn(II)tetraphenylporphyrine, ZnTPP, was prepared as previously published.<sup>8</sup> Purified MR was kindly provided by Professor K. Gollnick (Munich). Acetonitrile ( $CH_3CN$ ) and methanol ( $CH_3OH$ ) from Sintorgan, were of HPLC quality; toluene was from Merck (spectroscopic grade). Water was triply distilled.

\* Original reference *J. Photochem. Photobiol. B: Biology* (1993), 17, 247-255. Reproduced with kind permission of Elsevier Sequoia S.A.

## 2.2 Instrumentation and methods

Ground state absorption measurements were carried out with a Hewlett-Packard 8452A diode array spectrophotometer. For absorbance determinations at a fixed wavelength, a Shimadzu UV-140-01 spectrophotometer was employed. An Aminco SPF 125 spectrofluorometer was used for the steady-state fluorescence determinations. The excitation and emission wavelengths were, respectively, 480 and 535 nm for MR, and 275 and 355 nm for trp derivatives.

Fluorescence quantum yields ( $\Phi_f$ ) were determined using a computer-controlled Spex Fluorolog spectrofluorometer (excitation bandwidth 5 nm).<sup>9</sup> Eos was employed as a reference in water ( $\Phi_f = 0.11$ )<sup>5</sup>. Reference and sample absorbances were *ca.* 0.05 (1 cm pathlength) at 500 nm (excitation wavelength) and were matched to  $2 \times 10^{-3}$  absorbance units (bandwidth 5 nm).

Fluorescence lifetimes were measured by exciting the sample in a TRW 75A filterfluorometer with 5-ns pulses from a nitrogen laser. The signal from the photomultiplier was fed to a Hewlett-Packard 54200A digital oscilloscope and then to a PC computer for non linear least squares (time-shift) analysis and deconvolution.<sup>10,11</sup>

The laser flash photolysis apparatus has been previously described.<sup>12</sup> The second harmonic (532 nm) 15-ns pulse of a Nd:YAG laser (DPLY2, J. K. Lasers, Rugby, UK) was used to excite the solutions in a 1 cm<sup>2</sup> fluorescence quartz cuvette. The aqueous solutions were deoxygenated by bubbling ultra-pure N<sub>2</sub> during 30 min. Transient absorbance decays were fitted to a monoexponential decay plus a constant term.

The quantum yield for S → T intersystem crossing of MR in water was measured by laser flash photolysis and evaluated by the comparative method of Bensasson et al.<sup>13</sup> using ZnTPP in toluene as a reference ( $\lambda_{exc} = 532$  nm;  $A(532) = 0.104$ ;  $\lambda_{obs} = 470$  nm;  $\phi_{ISC} = 0.88$ ;  $\epsilon_T(470 \text{ nm}) = 74,000 \text{ M}^{-1} \text{ cm}^{-1}$ )<sup>14</sup>. For MR,  $A(532) = 0.101$ ;  $\lambda_{obs} = 500$  nm;  $\epsilon = 45,500 \text{ M}^{-1} \text{ cm}^{-1}$ .

The time resolved O<sub>2</sub>(<sup>1</sup>Δ<sub>g</sub>) phosphorescence-detection (TRPD) method used to determine the overall rate constants  $k_t$  for the interaction of the xanthene sensitizers (MR, Eos or RB) with O<sub>2</sub>(<sup>1</sup>Δ<sub>g</sub>) has already been described.<sup>15</sup> Briefly, it consisted of a Laser Optics nitrogen laser delivering 7-ns halfwidth and 5-mJ pulses (337 nm) as the excitation source. The emitted radiation (filtered with a Silicon filter  $\lambda > 1.05 \mu\text{m}$ ) was detected at right angles with an amplified Judson J16/8s Ge detector. The time constant of this system was *ca.* 4 μs. The output of the detector was coupled to a Gould Biomation (model 4500) digital oscilloscope and to a PC. Usually, an average of sixteen shots was needed in order to obtain a good signal to noise ratio.

For the determinations of  $\Phi_\Delta$  by TRPD in water, the second harmonic (532 nm) of a Nd:YAG laser (see above) and a North Coast cooled Ge-detector EO 817FP (200 ns time resolution) were used. RB was used as a reference ( $\Phi_\Delta = 0.75$ ).

The irradiation device for steady-state photolysis, including the specific oxygen electrode, was described elsewhere.<sup>16</sup> A cut-off filter for  $\lambda > 400$  nm was employed. In the determinations of  $\Phi_\Delta$  the specific oxygen electrode was coupled to a standard PTI photolyzer (75-W Xenon lamp). The irradiation slitwidth was 5 nm. All experiments were performed at  $20 \pm 2^\circ\text{C}$  (RT).

## 3. RESULTS

### 3.1. Dark complexation

The absorption spectrum of MR in water (Fig. 1 (a)) exhibits an intense absorption peak with maximum at 506 nm and molar absorption coefficient  $\epsilon = 45,500 \text{ M}^{-1} \text{ cm}^{-1}$  at pH = 7. In the presence of the amino acids trp and his, the absorption decreases in the blue edge of the visible band and in-

creases in its red edge. In methanolic solutions, the changes in the absorption spectra are similar (not shown). No changes were observed with gly, met, or ala. The concentrations of MR were kept  $< 10 \mu\text{M}$  in order to avoid possible aggregation. For all the amino acids, typical concentrations were in the order of  $10^{-3}$  M. The spectral changes could be better visualized by taking the difference spectra of the MR-amino acid system against MR under identical conditions as shown in the inset in Fig. 2. The presence of well defined isosbestic points is an indication that only two absorbing species are in equilibrium. Since the amino acids do not absorb in the visible, the species absorbing in the 500 nm region should be free MR and the complex MR-amino acid. Plotting the absorbance of the positive band vs. the amino acid concentration results in a saturation curve, as shown in Fig. 2. For trp-MR in water and in MeOH, and his in water, association constants ( $K_{ass}$ ) and molar absorption coefficients of the complexes ( $\epsilon$ ) were determined by the method of Rose and Drago (see ref. 17). The solid line in Fig. 2 shows the best fit obtained by this procedure for MR-trp at 530 nm. Similar plots were obtained for MR-trp in MeOH and MR-his in water. The values of  $K_{ass}$  and  $\epsilon$  at 530 nm for the systems MR-trp and MR-his are presented in Table I.

In order to elucidate the nature of the association, the sensitizer and the amino acid were varied. With other xanthene dyes, no spectral changes denoting any degree of association were observed, *e.g.*, for RB-trp and Eos-trp. On the other hand, with indole-3-acetic acid or tryptamine the spectral modifications of the MR solutions were qualitatively similar to those observed with trp.

Quenching of MR fluorescence intensity by amino acids was only detectable with those amino acids able to produce the spectral perturbations just described. The only effect produced by the addition of the amino acids was a decrease in the MR fluorescence intensity (Fig. 1). The Stern-Volmer plots for this decrease are linear up to amino acid concentrations of *ca.*  $3 \times 10^{-4}$  M (in Fig. 1, inset, the case of MR-trp is shown). At higher trp concentrations, the plot resembles a saturation curve. For trp and his in water, assuming that the fluorescence quenching does not proceed by dynamic quenching, the apparent association constants for complexation in the ground state should be calculated from the slopes of these plots.<sup>18</sup> The constants ( $K_{assf}$ ) thus obtained considering only the initial linear portion of the plots (Fig. 1) are also given in Table I. The values were similar although somehow always lower than those obtained by absorption (Table I).

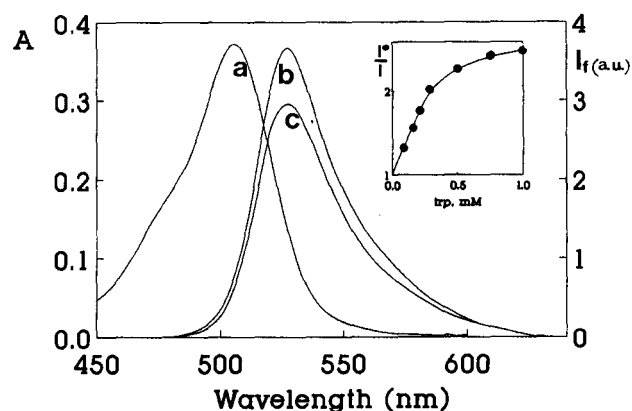


Figure 1. (a) Absorption (left) and (b) fluorescence spectra ( $I_f$ , right) of MR in water. (c) Fluorescence spectrum in the presence of 0.1 mM trp. Inset: Stern-Volmer plot for the quenching of MR fluorescence by trp ( $I^0$  and  $I$  represent the fluorescence intensity of MR in the absence and in the presence of trp, respectively).

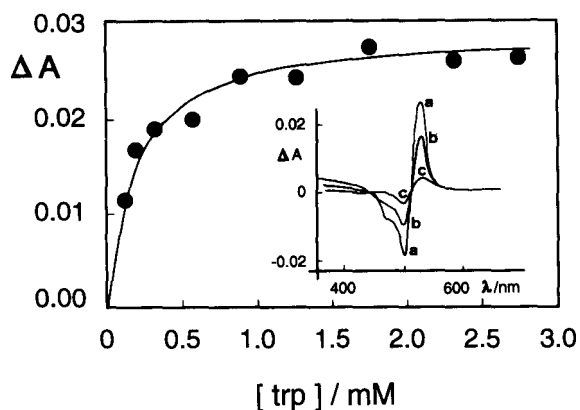


Figure 2. Absorbance at 530 nm as a function of trp concentration from the difference spectrum (MR vs. MR plus trp) shown in the inset, in water (pH = 7). (a) 0.3; (b) 0.18; and (c) 0.1 mM trp.

Table I. Association constants,  $K_{ass}$ , for the interaction between MR and amino acids in H<sub>2</sub>O or CH<sub>3</sub>OH, as determined by absorption and fluorescence and molar absorption ( $\epsilon$ ) for the complexes of MR and the various amino acids.

Amino acid/solvent	Absorption*		Fluorescence
	$K_{ass}^{\S}(M^{-1})$	$\epsilon^{\S}(M^{-1} cm^{-1})$	$K_{ass}(M^{-1})$
L-tryptophan/H <sub>2</sub> O	3600	27000	3400
L-tryptophan/MeOH	5000	29000	4600
L-histidine/H <sub>2</sub> O	3700	27300	3400

\*At 530 nm.

<sup>§</sup>Error in  $K_{ass}$  and in  $\epsilon$  is  $\pm 5\%$ .

### 3.2 Steady-state photolysis of RB and MR

Aerated aqueous solutions containing RB or MR, at matched absorbances ( $A(500)$  about 0.5 measured with a precision of 0.005; 5 nm bandwidth) were photolyzed at 500 nm, and the rates of dye consumption were monitored by the decrease in the maximum of the respective absorption spectrum. The products of the photodecomposition do not show absorption in the visible. The same results were obtained by monitoring the fluorescence intensities of the dyes upon irradiation. The former method was adopted for the quantitative evaluations. The rates of O<sub>2</sub> consumption for the solutions of the three dyes were determined under similar experimental conditions. Both sets of relative rates (O<sub>2</sub> uptake and dye consumption) are summarized in Table II. MR was by far the most photounstable dye. Note that the rate of O<sub>2</sub> consumption for MR was 15 times lower than the rate of dye consumption under the same experimental conditions. However, in N<sub>2</sub> saturated solutions, MR was bleached with the same rate as in O<sub>2</sub> saturated solutions.

Aqueous solutions ( $2 \times 10^{-5}$  M) of MR were irradiated in the visible absorption band ( $\lambda > 400$  nm) in the absence and in the presence of  $10^{-2}$  M NaN<sub>3</sub>. Within the experimental error, the rates of dye consumption were identical. The azide anion is commonly used as a probe for O<sub>2</sub>(<sup>1</sup> $\Delta_g$ ) ( $k_q = 2 \times 10^8$  M<sup>-1</sup> s<sup>-1</sup>).<sup>19</sup> A concentration of NaN<sub>3</sub> as large as that employed would have decreased the rate of MR consumption by a factor of ca. 20 in water (the decay rate constant of O<sub>2</sub>(<sup>1</sup> $\Delta_g$ ) in water is  $k_d = 2.5 \times 10^5$  s<sup>-1</sup>)<sup>20</sup>, should the main mechanism of such consumption be reaction with O<sub>2</sub>(<sup>1</sup> $\Delta_g$ ). The MR consumption in air saturated aqueous solutions containing 0.5 mM (CN)<sub>6</sub>Fe<sup>3-</sup> - a specific O<sub>2</sub> quencher<sup>21</sup> - was the same as in the aerated solutions.

Table II. Quantum yields for O<sub>2</sub>(<sup>1</sup> $\Delta_g$ ) generation ( $\Phi_{\Delta}$ ) and relative rates for consumption ( $R_s$ ) and oxygen uptake ( $R_{Ox}$ ) by MR, Eos and RB in water (buffer pH = 7) and rate constants for O<sub>2</sub>(<sup>1</sup> $\Delta_g$ ) quenching ( $k_t$  M<sup>-1</sup>s<sup>-1</sup>) by the dyes in CH<sub>3</sub>CN:H<sub>2</sub>O (1:1, v:v).

	$\Phi_{\Delta}$	$k_t \times 10^8$ CH <sub>3</sub> CN:H <sub>2</sub> O	$R_s$	$R_{Ox}$
xanthene				
MR	0.23	2.03	1	0.85
RB	0.75*	0.15	0.35	1
Eos	0.50 [0.51 <sup>§</sup> ]	0.27		

\*from [5], employed as a reference compound.

<sup>§</sup>from [5].

### 3.3 MR sensitized photooxidations

MR sensitized photooxidation of biomolecules frequently employed as targets for O<sub>2</sub>(<sup>1</sup> $\Delta_g$ )-photooxidative damage<sup>2</sup> were carried out. Aerated solutions of  $10^{-6}$  M MR with trp ( $2 \times 10^{-4}$  M in water) were irradiated with visible light. The changes in the fluorescence spectrum of trp document the sensitizing action of MR (Fig. 3A). Due to the high values of  $K_{ass}$  (Table I) CT complexation of MR with trp is almost quantitative at the low MR concentration used, whereas less than 1% of the trp molecules are complexed. The trp consumption was totally inhibited either in the presence of  $2 \times 10^{-2}$  M NaN<sub>3</sub> or when the solutions were saturated with N<sub>2</sub>.

The same effect was observed for met. Its consumption, upon irradiation of MR in its presence, was monitored by the decrease in the absorption band at 220 nm (data not shown).

For linoME, it is well established that a direct relationship can be obtained between the absorbance increase at 234 nm (due to the appearance of hydroperoxides of the fatty acids) and the degree of oxidation in the early stages of dye-sensitized oxygenation.<sup>22</sup> Photooxidation is interpreted in terms of a dual mechanism involving both O<sub>2</sub>(<sup>1</sup> $\Delta_g$ ) and radical attack on the double bonds. The sensitized oxidation can be neatly observed in Fig. 3B, for methanolic solutions of linoME at various concentrations.

### 3.4 Fluorescence

The fluorescence spectrum of MR in water at room temperature exhibited an intense band centered at 535 nm, as shown in Fig. 1 (b) (uncorrected). The fluorescence quantum yield in aerated water [Eos was employed as a reference] was  $\Phi_f = 0.19 \pm 0.03$  (Table III). The fluorescence lifetime was  $\tau_f = 3.4 \pm 0.2$  ns in N<sub>2</sub> and O<sub>2</sub> saturated solutions, and was practically the same ( $3.1 \pm 0.2$  ns) in CH<sub>3</sub>OH (in all cases the decay was monoexponential at least for 5 half-lives). The value of  $\tau_f$  was not affected by the presence of  $5 \times 10^{-3}$  M his, trp, or gly-trp. One should note, however, that assuming a diffusional quenching rate constant ( $k_q = 10^{10}$  M<sup>-1</sup> s<sup>-1</sup>) of <sup>1</sup>MR\* by the quenchers, for the O<sub>2</sub> concentration ( $10^{-3}$  M) or even for the highest amino acids concentration ( $5 \times 10^{-3}$  M), the perturbation in the value of  $\tau_f$  would be within the experimental error.

Table III. Quantum yield of fluorescence ( $\Phi_f$ ), intersystem ( $\Phi_{ISC}$ ), and O<sub>2</sub>(<sup>1</sup> $\Delta_g$ ) generation ( $\Phi_{\Delta}$ ), singlet ( $\tau_f$ ) and triplet ( $\tau_T$ ) excited state lifetimes for MR, and rate constant ( $k_q$ ) for the quenching of triplet MR by O<sub>2</sub>(<sup>3</sup> $\Sigma_g$ ) in water.

$\Phi_f$	$0.19 \pm 0.05$
$\Phi_{ISC}$	$0.23 \pm 0.03$
$\Phi_{\Delta}$	$0.23 \pm 0.04$
$\tau_f$	$3.4 \pm 0.02$ ns
$\tau_T$	$250 \pm 30$ $\mu$ s
$k_q$	$(1.1 \pm 0.5) \times 10^9$ M <sup>-1</sup> s <sup>-1</sup>

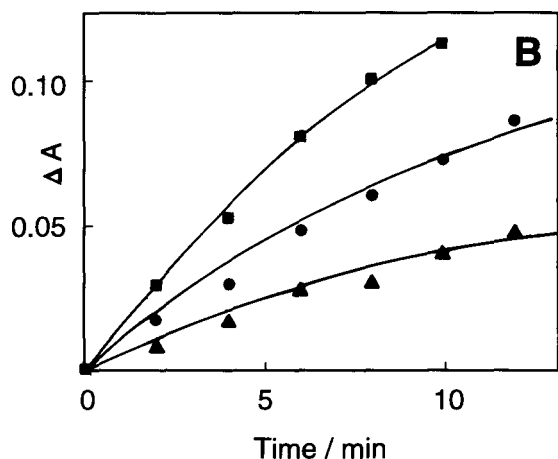
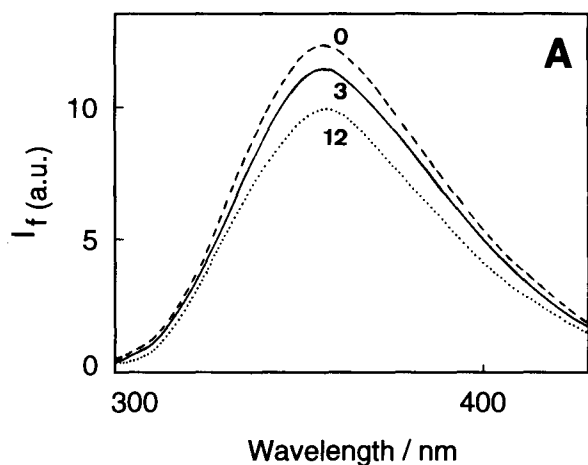


**Figure 3.** (A) Fluorescence spectra of  $2 \times 10^{-4}$  M trp aqueous solutions containing  $10^{-6}$  M MR as sensitizer, after irradiation with visible light (numbers represent the period of irradiation in minutes). (B) Photooxidation of methanol solutions of ( $\blacktriangle$ ) 10 mM, ( $\bullet$ ) 20 mM, and ( $\blacksquare$ ) 30 mM linol/ME using visible light and MR as sensitizer and monitored by the increase of absorbance at 234 nm.

### 3.5 Triplet state

The triplet state of MR was generated by direct excitation with a laser pulse at 532 nm and an energy of 4 mJ. It was not possible to obtain the T-S difference absorption spectrum (triplet minus singlet) in  $\text{CH}_3\text{OH}$  due to the rapid decomposition of the sample under irradiation. In water, the MR ground state spectrum remained unchanged for several laser shots. The sample was replaced by fresh MR solutions as soon as  $\Delta A$  at 500 nm was  $> 4\text{-}5\%$  due to dye decomposition, even in the absence of  $\text{O}_2$ . The T-S spectrum presents a broad absorption band from 550 to 700 nm (Fig. 4).

The MR triplet lifetime in water was  $\tau_t = 250 \pm 30 \mu\text{s}$ . The bleaching-recovery process showed a short-lived component ( $\lambda_{\text{obs}} < 530$  nm, lower curve in the inset of Fig. 4) the lifetime of which was equal to that of the triplet decay ( $\lambda_{\text{obs}} \geq 530$  nm, upper curve in the inset of Fig. 4). At longer times, the permanent bleaching was evident (see lower trace of inset).

The presence of trp or gly-trp up to  $10^{-2}$  M appreciably diminished the initial intensity of the difference absorbance, while no conclusion could be drawn about the influence on the decay due to the weakness of the signals.

A rough value for the bimolecular rate constant for the quenching of triplet MR by  $\text{O}_2(^3\Sigma_g^-)$  was estimated by measuring  $\tau_t$  in air and  $\text{N}_2$  saturated aqueous solutions. A value of

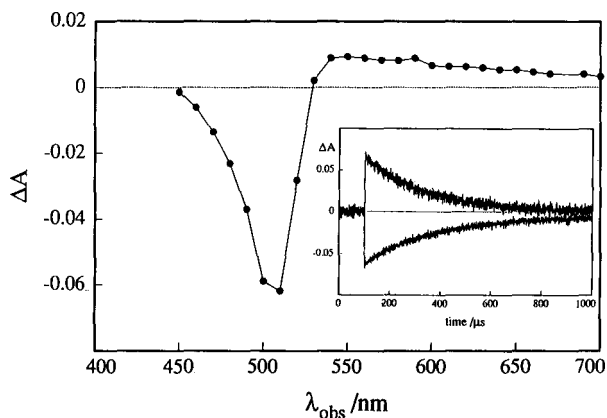


**Figure 4.** Difference absorption spectrum immediately after laser pulse ( $\lambda_{\text{exc}} = 532$  nm) excitation of MR in degassed aqueous solution (pH = 7). Inset: MR triplet decay at 590 nm (upper curve) and ground state bleaching recovery at 510 nm (lower curve).

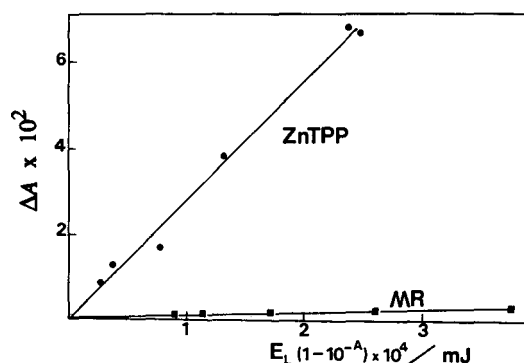


**Figure 5.** Absorbed-energy dependence of the transient-absorbance difference immediately after the laser pulse for MR in water ( $\lambda_{\text{obs}} = 590$  nm) and ZnTPP as a reference in toluene ( $\lambda_{\text{obs}} = 470$  nm).

$k_{\text{ET}} = 1.1 \pm 1 \times 10^9 \text{ M}^{-1} \text{ s}^{-1}$  was obtained using  $[\text{O}_2(^3\Sigma_g^-)] = 2.65 \times 10^{-4} \text{ M}$ .<sup>23</sup>

The changes in absorbance at zero time after the laser pulse vs. the laser energy absorbed by MR in water and by ZnTPP in toluene (used as reference) are plotted in Fig. 5. The comparison of the slopes yields a value of  $\Phi_{\text{ISC}} = 0.23 \pm 0.03$  for MR in water.

### 3.6 Determination of $\text{O}_2(^1\Delta_g)$ quenching

The values of the overall quenching rate constant of  $\text{O}_2(^1\Delta_g)$ ,  $k_t$ , by the dyes Eos, RB, and MR were determined by TRPD using the Stern-Volmer equation:  $\tau_{\Delta}^{\circ} / \tau_{\Delta} = 1 + k_t \tau_{\Delta}^{\circ} [\text{Q}]$ , where  $\tau_{\Delta}^{\circ}$  is the  $\text{O}_2(^1\Delta_g)$  lifetime which was measured employing AM as a sensitizer ( $\lambda_{\text{exc}} = 337$  nm) in  $\text{CH}_3\text{CN}:\text{H}_2\text{O}$  (1:1, v:v). This solvent mixture was chosen due to the limitation imposed by the low time resolution of the Ge detector used for these determinations, which impaired measurements in  $\text{H}_2\text{O}$  or in  $\text{CH}_3\text{OH}:\text{H}_2\text{O}$  mixtures.  $\tau_{\Delta}^{\circ}$  was constant (15  $\mu\text{s}$ ) in the AM concentration range  $5 \times 10^{-5} - 5 \times 10^{-4}$  M. The values of  $\tau_{\Delta}$  were obtained in the solvent mixtures employing the xanthene dyes (Q) as quenchers as well as sensitizers. From the slopes of  $\tau_{\Delta}^{\circ} / \tau_{\Delta}$  vs.  $[\text{Q}]$ ,  $k_t$  was derived (Table II). The decay curves of  $\text{O}_2(^1\Delta_g)$  emission, generated by AM and MR, and the Stern-Volmer plot for MR as quencher, are shown in Fig. 6.

### 3.7 Quantum yield for the generation of $O_2(^1\Delta_g)$ , $\Phi_\Delta$

Met is recognized as one of the five amino acids that effectively react with  $O_2(^1\Delta_g)$ .<sup>2</sup> Furthermore, the interaction is known to be entirely chemical with  $k_t = k_r = 2.1 \times 10^7 \text{ M}^{-1} \text{ s}^{-1}$ .<sup>24</sup> For this reason, we considered met as an adequate sacrificial substrate for the determination of  $\Phi_\Delta$  for the xanthene dyes.

Aqueous solutions (buffer pH = 7) of RB, and MR at matched absorbances  $A(500) = 0.3$ , were irradiated in the presence of  $2 \times 10^{-4} \text{ M}$  met. The rates of oxygen consumption (R), due to the reaction of met with  $O_2(^1\Delta_g)$ , were calculated from the slopes of the first order plots of  $\ln[O_2]$  vs. irradiation time (Fig. 7). Due to the high concentration of met, and to the low rate of  $O_2$  consumption in solutions of MR (*vide supra*),  $O_2$  consumption upon irradiation in this case can be considered only due to trapping of  $O_2(^1\Delta_g)$  by met. Employing RB as a reference ( $\Phi_\Delta = 0.76$ )<sup>5</sup>, the values of  $\Phi_\Delta$  for Eos and MR (Table II), were calculated using a comparative method with the following equation, in which  $R_x$  corresponds to the rate of oxygen consumption induced by each sensitizer:  $R_{RB}/R_x = \Phi_{RB}/\Phi_x$ . The determination of  $\Phi_\Delta$  in  $H_2O$  using the near-IR emission of  $O_2(^1\Delta_g)$  and a detector with a better time resolution, yields similar values (0.23 for MR and 0.51 for Eos, Table II).

Since the concentrations of RB, Eos, and MR were low (*ca.*  $10^{-6} \text{ M}$ ), even when the interaction of the dyes with  $O_2(^1\Delta_g)$  were purely chemical in nature (which is not), this reaction could be disregarded. This means that, under our experimental conditions, the contribution of the dyes to the process of  $O_2(^1\Delta_g)$  quenching is negligible, *i.e.*,  $k_t \text{ dye} [\text{dye}] \ll k_r [\text{met}]$ .

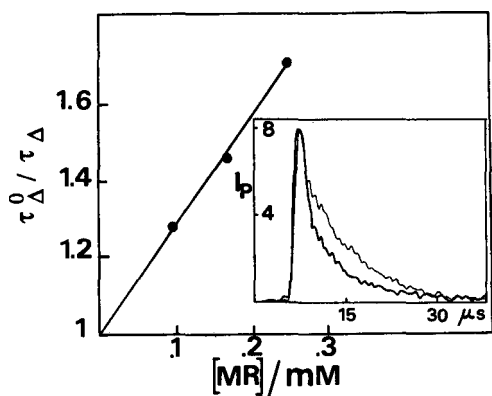


Figure 6. Stern-Volmer plot for the quenching of  $O_2(^1\Delta_g)$  luminescence by MR, in  $CH_3CN:H_2O$  (1:1, v:v). Inset: decay of  $O_2(^1\Delta_g)$  emission, upper curve: generated by 0.4 mM AM ( $\lambda_{exc} = 337 \text{ nm}$ ), lower curve: generated by 0.18 nM MR ( $\lambda_{exc} = 337 \text{ nm}$ ).

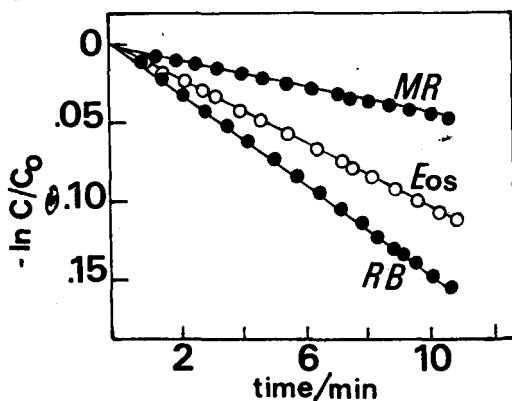
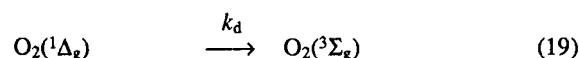
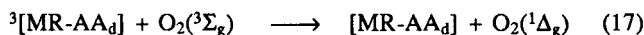
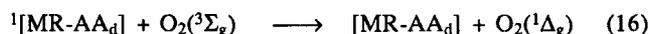
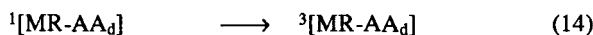
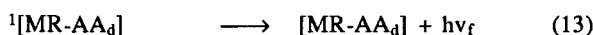
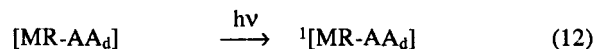
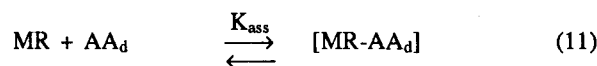
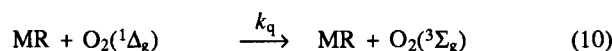
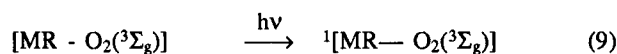
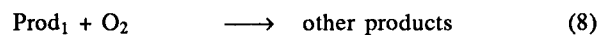
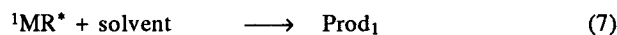
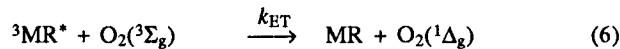
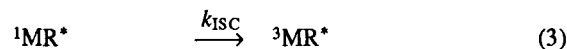
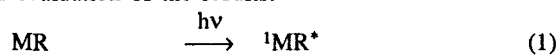


Figure 7. First-order plots for  $O_2$  uptake by irradiated aqueous solutions of the dyes (*ca.*  $10^{-6} \text{ M}$ , matched absorbances at 500 nm) in the presence of  $2 \times 10^{-4} \text{ M}$  met.  $C_0$  and  $C$  are  $[O_2]$  at time zero and  $t$ , respectively.

### 4. DISCUSSION

The following reaction scheme is employed for presentation and evaluation of the results:



where AA represents all amino acids, while  $\text{AA}_d$  represents those with high electron donor ability leading to the formation of CT complexes. Reference to the various equations will be made in the following discussion.

#### 4.1 Dark association

J. Chrysochoos in 1974 described the association of organic electron donors, such as aromatic amines and pyridine, with the xanthene dye Eos.<sup>25</sup> The author postulated that the intermolecular association was probably governed by contributions from several interactions such as hydrogen bond, charge-dipole, and charge-transfer processes, with Eos acting as an electron acceptor. The spectral changes due to the association are very similar in shape to those described in the present work for the system MR-indole derivatives and MR-his. The most important difference between the work of Chrysochoos on Eos complexes and our results on MR is the magnitude of the association constant,  $K_{ass}$  (eq. 11), being for MR between two and three orders of magnitude higher. In agreement with former proposals for the cases of dark complexation of the electron acceptor riboflavin with imidazole and indole derivatives,<sup>18</sup> we assume that the associations MR-indoles and MR-his are mainly driven by a charge transfer (CT) mechanism. Indoles have an extended  $\pi$ -electron system and possess an electron rich heteronuclear ring. Consequently, both types of compounds should be able to form highly stable molecular

complexes with ground state electron acceptors. This is supported by the absence of ground state interaction of MR with the aliphatic amino acids ala, met and gly, demonstrating that the presence of the amino group is not the only factor determining the formation of relatively high-stable complexes, such as those with trp and his.

Similar to the case of the Eos complexes,<sup>25</sup>  $K_{ass}$  was higher in methanol than in water solutions. This can be rationalized considering the presence of the ionized form of MR in water and the predominance of the MR neutral form in  $CH_3OH$ . The dye should thus exhibit better acceptor character in the organic solvent.

The reduction of MR steady-state fluorescence by the amino acids and the similarity between the  $K_{ass}$  values, as determined by absorption and fluorescence methods, together with the photolysis results, indicate that the ground state CT complexes are responsible for the photoreaction in the case of strong electron donor amino acids (eq. 11) and that static quenching of  $^1MR^*$  by the amino acids plays an important role.

For the donor amino acids studied, the absorption coefficients of the complexes are similar, within experimental error (Table I). The saturation effect in the Stern-Volmer plots (Fig. 1) results from the complex mechanism implying fluorescence from  $^1MR^*$ , from the CT complex, (with a fluorescence spectrum very similar to that of  $^1MR^*$ , Fig. 1) and quenching by the amino acids in excess (eq. 15) which is negligible at low quencher concentration (*i.e.*, when the Stern-Volmer slope is equal to  $K_{ass}$ ) and becomes important as the complex concentration increases.

#### 4.2. Photophysics of MR and its interaction with $O_2(^3\Sigma_g^-)$ and $O_2(^1\Delta_g)$

In water, the MR first excited singlet state fluoresces strongly (for quantum yields and lifetimes see Table III). The fluorescence spectrum approximates mirror symmetry with the lowest energy absorption transitions (Fig. 1) and the excited singlet possesses a lifetime of the same order as those for other xanthene derivatives.<sup>5</sup> Intersystem crossing to the triplet manifold (eq. 3) occurs with  $\Phi_{ISC} = 0.23 \pm 0.05$  and the value of  $\tau_1 = 250 \pm 30 \mu s$  makes it easily quenchable by  $O_2$  at low concentrations (eq. 6, see Table III). One should expect, due to the internal heavy atom effect of mercury,<sup>26</sup> a much higher  $\Phi_{ISC}$  for MR, specially taking into account the value of  $\Phi_f = 0.19$  (Table III) determined under the same conditions. The same problem was discussed by Gollnick *et al.*<sup>7</sup> for MR in  $C_2H_5OH$ , except that no information about  $\Phi_f$  was available to these authors. In our case, even allowing for higher experimental uncertainties in the fluorescence and intersystem crossing determinations, internal conversion (eq. 4) from the first excited to the ground state and reaction from the excited singlet are the dominant deactivating processes.

In the absence of  $O_2(^3\Sigma_g^-)$ , the complete return of the triplet to the ground state, in addition to the fact that MR photobleaches with the same rate in the presence or in the absence of  $O_2$ , supports the concept that the photobleaching of MR is due to a reaction of its singlet excited state. The value of the rate constant for quenching of the MR triplet by  $O_2(^3\Sigma_g^-)$  (eq. 6) in water ( $k_q = 1.1 \pm 0.5 \times 10^9 M^{-1} s^{-1}$ ) is in good agreement with that reported by Lee and Rodgers ( $1.6 \times 10^9 M^{-1} s^{-1}$ )<sup>27</sup> for the same process involving RB.

The formation of  $O_2(^1\Delta_g)$  via triplet quenching (eq. 6) was previously reported by Gollnick *et al.* for MR<sup>6,7</sup> in  $CH_3OH$  and  $C_2H_5OH$ . The  $\Phi_\Delta$  values were estimated as 0.1 and 0.14, respectively, with  $\Phi_{ISC} = 0.16$  in the latter solvent.<sup>7</sup> In water, we obtained higher values (0.23) both for  $\Phi_\Delta$  and  $\Phi_{ISC}$  (Table III). In this case, the efficiency of  $O_2(^1\Delta_g)$  generation is  $S_\Delta = 1$ , as calculated from the relationship  $\Phi_\Delta = \Phi_{ISC} \times S_\Delta$ .

MR, in turn, is an efficient  $O_2(^1\Delta_g)$  quencher in

$CH_3CN:H_2O$  mixtures as (Table II). In  $H_2O$  or in alcohol: $H_2O$  mixtures, MR should be an equally efficient  $O_2(^1\Delta_g)$  quencher. The value of  $k_t$  is significantly higher than that obtained under similar conditions for RB and Eos (Table II). Since under steady state irradiations the MR consumption in air-saturated solutions was the same in the presence and in the absence of  $10^{-2} M NaN_3$ , the rate constant of  $O_2(^1\Delta_g)$  quenching ( $k_q = 2.03 \times 10^8 M^{-1} s^{-1}$ ,  $k_t = k_q$ , eq. 10).

Since under steady-state irradiation the MR photobleaching was the same in air as in  $N_2$ -saturated solutions, the photobleaching of MR most probably involves the (solvent (eq. 7). This is supported by the fact that in alcoholic solutions MR consumption was faster than in aqueous solutions (data not shown). The oxygen consumption during the photobleaching of MR solutions without additives should thus be attributed to the reaction of  $O_2$ , with the initial labile products of the MR photolysis (eq. 8).

The quenching rate constants of  $O_2(^1\Delta_g)$  by Rb and Eos are in the same range as those reported by Tanielian *et al.*<sup>28</sup> in pure  $CH_3CN$  (Table II). The authors determined  $k_t$  by competition kinetics between 2-methyl-2-pentene and the dye sensitizers, but since no analysis of the disappearance of the dyes was performed, no discrimination about the relative importance of  $k_q$  and  $k_r$  could be made. Lee and Rodgers reported that the photosensitized bleaching observed in aqueous RB solutions was mainly due to destruction by  $O_2(^1\Delta_g)$  though an oxygen-independent bleaching reaction could also operate.<sup>27</sup>

In conclusion, MR photobleaching should be attributed to a singlet mechanism without participation of  $O_2(^1\Delta_g)$  or  $O_2^-$ , whereas RB photobleaching is due mainly to self sensitized destruction by  $O_2(^1\Delta_g)$ . In addition, there is a large difference in the values of  $\Phi_\Delta$  for both dyes (Table II). Thus, the mechanisms of the photochemical behavior of these two dyes are entirely different.

#### 4.3. Amino acid bleaching photosensitized by MR

The photobleaching of donor amino acids in the presence of MR should be interpreted as a reaction of the ground state CT complexes with the participation of  $O_2(^1\Delta_g)$  produced by interaction of  $O_2(^3\Sigma_g^-)$  with either the singlet or the triplet state of the complex (eqs. 16 and 17). This is supported by the inhibitory effect of  $N_3Na$  and the absence of photobleaching in the presence of  $N_2$ . An interaction of  $^1MR^*$  with the amino acids cannot be totally discarded since the large error involved in the determination of the relatively short value of  $\tau_f$  impaired the evaluation of a possible influence of additives. However, neither the physical quenching of  $O_2(^1\Delta_g)$  by MR nor any interaction of amino acids with free MR (singlet or triplet) could compete favourably with moderately efficient biological quenchers of  $O_2(^1\Delta_g)$ , due to the low concentration of the dye under sensitizing conditions.

In the case of aliphatic amino acids (met) and unsaturated fats (e.g. linoME), the photodynamic action of MR operates through a typical type II mechanism involving  $O_2(^1\Delta_g)$  generated by triplet MR (eq. 6 followed by eq. 18).

#### ACKNOWLEDGEMENTS

Thanks are given to Consejo Nacional de Investigaciones Científicas Técnicas (CONICET, República Argentina), Consejo de Investigaciones de Córdoba (CONICOR, Provincia de Córdoba, Argentina), Universidad Nacional de Río Cuarto (UNRC, Río Cuarto, Argentina) and Bundesministerium für Forschung und Technology (BMFT, Verbundstudie Photodynamische lasertherapie, Germany) for partial financial support. The interest and support of Professor K. Schaffner is acknowledged. N. A. G. thanks Professor Klaus Gollnick (Germany) for encouraging this work.

## REFERENCES

1. Koizumi, M.; Kato, S.; Mataga, N.; Matsuura, T.; Isui, I.; *Photosensitized Reactions*, Kagakudogin Pub. Co., Kyoto, (1978).
2. Straight, R. C.; Spikes, J. D.; In *Singlet O<sub>2</sub>*, Vol. IV, Frimer, A. A.; Ed. CRC Press. Boca Raton, (1985).
3. Wilkinson, F.; Brummer, J. G.; *J. Phys. Chem. Ref. Data* (1981), **10**, 809.
4. Foote, C. S. In *Photosensitization*, Moreno, G.; Pottier, R. H.; Truscott, T. G. Eds. NATO ASI Series, Series H: Cell Biology, **15**, Springer-Verlag, Berlin, (1988).
5. Neckers, D. C.; *J. Photochem. Photobiol., A: Chemistry* (1989), **47**, 1.
6. Gollnick K.; Held, S.; *J. Photochem. Photobiol., B: Biology* (1990), **5**, 85.
7. Gollnick, K.; Franken, T.; Fouda, M. F. R.; Paur, H. R.; Held, S. *J. Photochem. Photobiol., B: Biology* (1992), **12**, 57.
8. Rossbroich, G.; García, N. A.; Braslavsky, S. E.; *J. Photochem.* (1985), **31**, 37.
9. Holzwarth, A. R.; Lehner, H.; Braslavsky, S. E.; Schaffner, K.; *Liebigs Ann. Chem.* (1978), 2002.
10. Demas, J. N.; *Excited States Lifetime Measurements*, Academic Press, New York, (1983).
11. Knight, A. E. W.; Selinger, B. K.; *Austr. J. Chem.* (1973), **26**, 1.
12. Ruzsicska, B. P.; Braslavsky, S. E.; Schaffner, K. *Photochem. Photobiol.* (1985), **41**, 681.
13. Bensasson, R. V.; Goldschmidt, C. R.; Land, E. J.; Truscott, T. G.; *Photochem. Photobiol.* (1978), **28**, 277.
14. Carmichael, I.; Hug, G. L.; *J. Phys. Chem. Ref. Data* (1986), **15**, 183.
15. Bertolotti, S. G.; García, N. A.; Argüello, G.; *J. Photochem. Photobiol., B: Biology* (1991), **10**, 57.
16. Palumbo, M. C.; García, N. A.; Argüello, G.; *J. Photochem. Photobiol., B: Biology* (1990), **7**, 33.
17. Foster, R. *Organic Charge Transfer Complexes*, Chap. 6, Academic Press, New York, (1969).
18. Slifkin, M. *Charge Transfer Interactions of Biomolecules* Chap. 7, Academic Press, London, (1971).
19. Kraljic, I.; Sharpatyi, V. A.; *Photochem. Photobiol.* (1978), **28**, 583.
20. Rodgers, M. A. J.; *J. Am. Chem. Soc.* (1983), **105**, 6201.
21. Giulivi, C.; Sareansky, M.; Rosenteld, E.; Boveris, A.; *Photochem. Photobiol.*, (1990), **52**, 745.
22. Nawar, W. in *Food chemistry*, Chap. 4, 2nd. edition Fennema O. R. Ed., Marcel Dekker, New York, (1985).
23. Murov, S. L.; *Handbook of Photochemistry*, Chap. 9, Marcel Dekker, Inc., New York, (1973).
24. Lindig, B. A.; Rodgers, M. A. J.; *Photochem. Photobiol.* (1981), **33**, 627.
25. Chrysochoos, J.; *Mol. Photochem.*, (1974), **6**, 23.
26. McGlynn, S. P.; Azumi, T.; Kinoshita, M.; *Molecular Spectroscopy of the Triplet State*, Prentice Hall, Englewood Cliffs (1969).
27. Lee, P. C. C.; Rodgers, M. A. J.; *Photochem. Photobiol.*, (1987), **45**, 79.
28. Tanielian, C.; Golder, L.; Wolff, C.; *J. Photochem.* (1984), **25**, 117.

*This special issue of Química Nova is dedicated to Prof. G. Cilento on the occasion of his 70<sup>th</sup> birthday and is financed by the Fundação de Amparo à Pesquisa do Estado de São Paulo (FAPESP).*